

Simulation of an inhomogeneous Fermi gas through the BCS-BEC crossover

R. Jáuregui, R. Paredes, L. Rosales-Zárate, and G. Toledo Sánchez

*Departamento de Física Teórica, Instituto de Física,
Universidad Nacional Autónoma de México, A.P. 20-364, México 01000 D.F. México*

(Dated: November 29, 2008)

We perform a variational quantum Monte Carlo simulation of the transition from a Bardeen-Cooper-Schrieffer superfluid (BCS) to a Bose-Einstein condensate (BEC) at zero temperature. The model Hamiltonian involves an attractive short range two body interaction and the atoms number $2N = 330$ is chosen so that, in the non-interacting limit, the ground state function corresponds to a closed shell configuration. The system is then characterized by the s -wave scattering length a of the two-particle collisions in the gas, which is varied from negative to positive values, and the Fermi wave number k_F . Based on an extensive analysis of the s -wave two-body problem, one parameter variational many-body wave functions are proposed to describe the ground state of the interacting Fermi gas from BCS to BEC states. We exploit properties of antisymmetrized many-body functions to develop efficient techniques that permit variational calculations for a large number of particles. It is shown that a virial relation between the energy per particle and the trapping energy is approximately valid for $-0.1 < 1/k_F a < 3.4$. The influence of the harmonic trap and the interaction potential as exhibited in two-body correlation functions is also analyzed.

I. INTRODUCTION

The experimental realization of a degenerate Fermi gas in 1999¹, boosted theoretical and experimental efforts to study interacting Fermi gases, in particular, the formation of molecules and highly correlated pairs from a balanced mixture of neutral interacting Fermi atoms in two different hyperfine spin states^{2,3,4,5,6,7}. The possibility of tuning the strength of the interaction between particles in different spin states via Feshbach resonances, results in the formation of Cooper pairs (molecules) for negative (positive) values of the scattering length a . At low temperatures, these pairs and molecules can form a Bardeen-Cooper-Schrieffer (BCS) superfluid state and a Bose-Einstein condensate (BEC) respectively. When crossing from the BCS to the BEC region, and viceversa, a grows in magnitude until it diverges at the resonance. In this limit the scattering length is no longer a relevant scale, and the properties of the gas become independent of the specific details of the interaction potential. This is the so called unitarity limit in which the gas is assumed to be universal^{3,7,8,9}, because its properties depend locally just on the density and the temperature, i.e., the only relevant scales in this quantum gas are the interparticle spacing and the Fermi energy. Consequently the gas properties can be expressed in terms of them and universal parameters^{3,7,8}.

Previous treatments of the BCS-BEC crossover in degenerate atomic gases have been done using different approaches, we can mention the self-consistent many-body approach⁷, the effective field theory¹⁰, and more recently quantum Monte Carlo calculations^{11,12,13,14,15,16,17}. This last treatment has been predominantly based on the fixed node Quantum Monte Carlo technique. In most of these calculations, the two-component Fermi gas is considered as an homogeneous system although, experimentally, the gas has an intrinsic inhomogeneous nature provided usually by a magnetic and/or optical trap. Such confining can be described by a harmonic potential. An interesting parameter calculated in those approaches is β , which relates the Fermi energy of the ideal Fermi gas E_{IFG} and the total energy of the interacting gas E . This parameter is expected to acquire a universal value at unitarity⁸. The predicted values for β ranges from -0.75 to -0.33^{7,10,11,13,14}. First experimental estimates gave $\beta \sim -0.36^5$ and $\beta \sim -0.49 \pm 0.04^{18}$ while, more recently, values around $-0.54^{19,20}$ have been reported. The later results are based on measurements of the gas cloud radii at unitarity.

In a recent work²¹, we employed variational quantum Monte Carlo techniques (VQMC) to describe a balanced two-component interacting gas confined in a three-dimensional harmonic potential. There, we reported direct tests of the universality hypothesis in the unitarity limit that include: (i) the verification of virial relations for $N = 4, 10, 20, 35, 56, 84, 120, 165$ and 220 , (ii) the variational estimate $\beta_{fit} \geq -0.50^{(+0.02)}_{(-0.04)}$ using a linear fit of the energy per particle. In that paper we also briefly reported an analysis on observables like the system energy and density profiles in the BCS-BEC crossover. In particular we found N -independent energy curve features through the crossover.

In the present article, we extend the analysis of Ref.²¹, paying special attention to exhibit additional properties of the trial many-body wave functions, whose structure incorporates, in an analytic and compact form, important features of the trapped two-body system. Particular properties of the antisymmetrized many-body functions, let us develop efficient techniques that permit variational calculations for an unusual large number of particles. The optimized wave functions allow the study of the influence of the harmonic trap and the interaction potential in energies, densities and two-body correlation functions, all along the crossover. The correlations between atoms in the same hyperfine state

show the Pauli-blocking evolution as a function of a . Similarly, the correlations for atoms in different hyperfine states give information on the formation of molecules and Cooper pairs. The applicability of virial relations to our results is also analyzed. Here we report results for $N = 165$ particles per each hyperfine state.

This work is organized as follows: in section II, an extensive discussion of the two-body problem in the trap is done, and expressions for two-body functions that contain interaction and trap effects are obtained. The results of that section are then used to construct variational many-body wave functions for each region of the crossover. In section III, we address the many-body system and exploit the structure of the variational wave functions to optimize numerical calculations. There, we describe in detail the procedure for the variational quantum Monte Carlo simulation and energy evaluation. This section also contains the results for optimal variational parameters and energies, as well as densities and two-body correlation profiles. Our conclusions are presented in section IV.

II. THE TWO-BODY PROBLEM

In this section we shall establish the two-particle system features. As it is well known, in the limit of low energies it is expected that the scattering process, represented by the s -wave scattering length a , determines the general features of the state of two colliding particles, regardless the detailed form of the interaction potential among them.

Here we consider two particles of mass m trapped in a harmonic potential of frequency ω and interacting through an isotropic attractive potential of finite range $b/2$ given by

$$V(r_{i,j}) = V_0 e^{-2|\mathbf{r}_{i\uparrow} - \mathbf{r}_{j\downarrow}|/b}, \quad V_0 < 0 \quad (1)$$

where the \uparrow and \downarrow subindices denote two different hyperfine atomic states and $b \ll \sqrt{\hbar/m\omega}$. The potential is chosen so that, in otherwise free space, it would admit a finite number of bound states as its strength V_0 is varied.

For interactions taking place in free space, the Schrödinger equation

$$\left[\frac{p^2}{m} + V\right]\phi = \mathcal{E}\phi \quad (2)$$

has analytical s -wave solutions²³ $\phi(r) = v(r)/r$ both in the continuum

$$v(y) = c_1 J_{ib\sqrt{\mathcal{E}m}/\hbar}(y) + c_2 J_{-ib\sqrt{\mathcal{E}m}/\hbar}(y), \quad (3)$$

and in the bound states region

$$v(y) = c_+ J_{b\sqrt{|\mathcal{E}|m}/\hbar}(y) \quad (4)$$

where $y = \zeta e^{-r/b}$, $\zeta = (b\sqrt{|V_0|m}/\hbar)$, and J_ν represents the Bessel function of the first kind of order ν . By imposing the proper boundary conditions and considering the limit $\mathcal{E} \rightarrow 0^+$, the following expression is found for the s -wave scattering length dependent just on ζ

$$a = -b \left[\frac{\pi}{2} \frac{N_0(\zeta)}{J_0(\zeta)} - \log(\zeta/2) - C \right], \quad (5)$$

with N_0 the Bessel function of the second kind and order zero, and C the Euler constant. This scattering length diverges whenever $J_0(\zeta) = 0$. Denoting the zeros of the J_0 Bessel function in increasing order by z_k ($k = 0, 1, 2, \dots$), the potential $V(r)$ admits just k -bound states for $z_k < \zeta < z_{k+1}$. The discrete eigenvalues are determined by the boundary condition at $r = 0$, $J_{b\sqrt{|\mathcal{E}|m}/\hbar}(b\sqrt{|V_0|m}/\hbar) = 0$.

When the two-body collision process takes place in the presence of an isotropic harmonic potential, the two-body Schrödinger equation can be separated in a center of mass equation

$$\left[\frac{P_{CM}^2}{2M} + \frac{1}{2}M\omega^2 R_{CM}^2\right]\Phi(\mathbf{R}_{CM}) = E_{CM}\Phi(\mathbf{R}_{CM}), \quad (6)$$

and a relative coordinate equation

$$\left[\frac{p^2}{2\mu} + \frac{1}{2}\mu\omega^2 r^2 + V(r)\right]\varphi(\mathbf{r}) = \epsilon\varphi(\mathbf{r}). \quad (7)$$

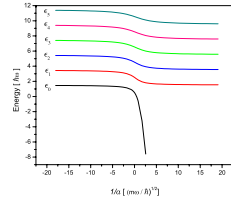


FIG. 1: (Color online) Lowest s -wave relative energy eigenvalues in units of $\hbar\omega$ for two colliding trapped particles, Eq. (7), around the first resonance. It was evaluated by considering a potential range $b/2 = 0.015\sqrt{\hbar/m\omega}$ and a strength V_0 starting from $V_0 \sim 0$ to the lowest $|V_0|$ yielding $a \rightarrow 0^+$. The scattering length is measured in units of $\sqrt{\hbar/m\omega}$.

with $\mu = m/2$ and $M = 2m$. The former is the isotropic harmonic oscillator equation whose solutions are well known, and the latter can be numerically solved given b and V_0 .

Figure 1 illustrates the s -wave lowest eigenvalues ϵ_n , $n \leq 5$, as a function of the inverse of the scattering length when the potential parameters are in the first resonance region ($\zeta = b\sqrt{|V_0|m/\hbar}$ around z_0) and $b \ll \sqrt{\hbar/m\omega}$. For $-\infty < 1/a < 0$, the spectrum is discrete with positive values in counterpart to the free space system which has a continuum spectrum and no bound states. In fact for $a \rightarrow 0^-$, $\epsilon_n \cong (2n + 3/2)\hbar\omega$ as expected. At resonance, $1/a = 0$, the ground state energy $\epsilon_0 \sim 1/2\hbar\omega$. For positive a , ϵ_0 decreases becoming zero at $1/a \sim 1/2\sqrt{\hbar/m\omega}$. For $a \rightarrow 0^+$, ϵ_0 takes values close to the ground state energy of the free space system, Eq. (2), while the excited states energies become $\epsilon_{n>0} \cong (2n - 1/2)\hbar\omega$. In the whole region $-\infty < 1/a < \infty$, all $\epsilon_{n>0}$ exhibit a similar behavior and are consecutively spaced among them by a factor of $\sim 2\hbar\omega$. In fact, at resonance, $\epsilon_n \cong (2n + 1/2)\hbar\omega$.

If ζ is further increased, the scattering length becomes negative until the second resonance is reached at z_1 . Around the second resonance, the eigenvalue ϵ_{t+1} as a function of a is similar to ϵ_t around the first resonance. For instance, for $\zeta = z_1$, the *first* excited state energy ϵ_1 becomes $\epsilon_1 \cong \hbar\omega/2$. Meanwhile, the ground state energy ϵ_0 remains similar to the corresponding ground state energy of Eq. (2) which decreases with growing ζ . Higher values of ζ yield analogous results, so that ϵ_{k+t} , $t = 0, 1, 2, \dots$ as a function of $1/a$ around the $(k+1)^{th}$ -resonance is similar to ϵ_t around the first resonance.

As expected, the qualitative behavior of the spectrum illustrated in Fig. 1 using the finite range interaction V , is in excellent agreement with the analytical results for two harmonically trapped particles interacting through a regularized contact potential $(4\pi\hbar^2 a/m)\delta_{reg}(\mathbf{r}_i - \mathbf{r}_j)^{24}$. For that problem, Busch *et al* found an implicit equation for the energy eigenvalues ϵ ,

$$\sqrt{2} \frac{\Gamma(-\epsilon/(2\hbar\omega) + 3/4)}{\Gamma(-\epsilon/(2\hbar\omega) + 1/4)} = \frac{\sqrt{\hbar/m\omega}}{a}, \quad (8)$$

and the explicit expression for the corresponding eigenfunctions. In particular, for $|a| \rightarrow \infty$, the ground state energy is $\epsilon_0 = \hbar\omega/2$. We have checked that given a , the finite range interaction spectrum ϵ_{k+t} , $t = 0, 1, 2, \dots$ around the $(k+1)^{th}$ -resonance reproduces with increasing accuracy the contact interaction spectrum as the potential range parameter $b \rightarrow 0$. In order to obtain such matching, shorter potential ranges $b/2$ are required for negative energies

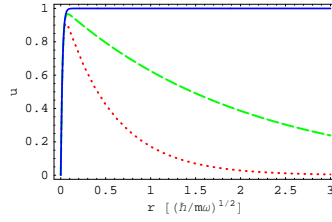


FIG. 2: (Color online) Radial function $u_a(r)$ for interacting particles in otherwise free space. The zero-energy resonant function $u_\infty(r)$ (solid line) tends to a nonzero constant as $r \rightarrow \infty$, meanwhile $u_{2.1}(r)$ (dashed line) and $u_{0.58}(r)$ (dotted line) correspond to increasingly bound states. Distances are measured in units of $\sqrt{\hbar/m\omega}$.

than for positive energies.

From now on, we consider just short range potentials and ζ around the first resonance condition. The general behavior of the s -ground state eigenfunctions $\varphi_a(r)$ is illustrated in Fig. 2 and Fig. 3 in terms of the functions u_a ($\varphi_a(r) = u_a(r)/r$) considering the free space and trapped system respectively. In both figures, the solid line represents u_∞ at resonance ($a = \infty$). The structure of this ground state trapped wave function deviates significantly from its free-space analog not just at long distances but also near the origin.

For $a < 0$, we have found that the numerical solution can be approximated using the following analytical compact representation:

$$\varphi_{apx}(r) = J_0(z_0 e^{-r/b}) e^{-m\omega r^2/4\hbar} (1 + c e^{-2r/b}) P(r/b)/r \quad (9)$$

where c is independent of r and $P(r/b)$ is a polynomial function. In fact, this approximation has an accuracy higher than 0.01% by the proper choice of c and a fourth order polynomial $P(r/b)$, both of which depend on V_0 and b . The accuracy of this approximation was measured by evaluating the ratio $\varphi_{apx}(r)/\varphi_{num}(r)$ between the analytical approximate expression Eq. (9) and the numerical solution.

For $\zeta > z_0$ in the region of positive a , the *ansatz* for the ground state function is:

$$\varphi_{apx}(r) = v(y(r)) e^{-m\omega r^2/4\hbar} g(r)/r \quad (10)$$

where v was defined in Eq. (4). The function φ_{apx} is numerically accurate at least at the 1% level. Its structure let us understand the origin of the eigenvalue $\epsilon \sim 1/2\hbar\omega$. In this case, $v(y(r))$ takes care of the boundary condition $v(0) = 0$ so that the effective equation for $g(r)$ is almost identical to its analog for the one dimensional harmonic oscillator without the requirement of becoming null at $r = 0$, thus admitting the possibility $\epsilon = \hbar\omega/2$.

The analytical approximations given by Eqs(9-10) to the exact solutions of the two-body problem will be exploited in the study of the many-body system.

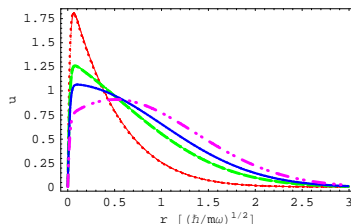


FIG. 3: (Color online) Radial function $u_a(r)$ for interacting particles in the presence of the trapping potential. The dot-dashed curve corresponds to the ground s -state for a negative scattering length $u_{-0.6}(r)$, the resonant function $u_{\infty}(r)$ is given by the solid curve, while $u_{2.1}(r)$ by the dashed one and $u_{0.58}(r)$ by the dotted line. In this figure the wave functions have been properly normalized. Distances are measured in units of $\sqrt{\hbar/m\omega}$.

III. THE MANY-BODY SYSTEM

Let us consider the system made up of $2N$ fermions of mass m in two, equally populated, hyperfine states ($N_{\uparrow} = N_{\downarrow}$) confined in an isotropic three-dimensional harmonic trap of frequency ω . The system is allowed to interact via collisions between particles of different hyperfine states. The Fermi gas is considered to be at zero temperature and the two-body collision process is approximated by the single-channel model described in the previous section, Eq. (1). The Hamiltonian describing such a system is:

$$H = H_{trap} + \sum_{i,j} V(r_{i,j})$$

$$= \sum_{i,j=1}^N \left[\frac{p_{i\uparrow}^2 + p_{j\downarrow}^2}{2m} + \frac{1}{2} m \omega^2 (r_{i\uparrow}^2 + r_{j\downarrow}^2) \right] + \sum_{i,j=1}^N V(|\mathbf{r}_{i\uparrow} - \mathbf{r}_{j\downarrow}|) \quad (11)$$

$$(12)$$

A. Variational Monte-Carlo simulations

In a variational calculation, for a given form of the interaction potential, the optimal value of any variational parameter λ in the wave function Ψ_{λ} , is determined by imposing that the expectation value of the Hamiltonian, Eq. (12) in our problem, to be a minimum with respect to such parameter. So that,

$$\frac{\partial E(\lambda)}{\partial \lambda} = 0, \text{ where } E(\lambda) = \frac{\langle \Psi_{\lambda} | H | \Psi_{\lambda} \rangle}{\langle \Psi_{\lambda} | \Psi_{\lambda} \rangle}. \quad (13)$$

For a system of $2N$ atoms, computing the expectation value requires the evaluation of a $6N$ -dimensional integral. The main idea of the Monte Carlo method³² is not to evaluate the integrand at every one of the quadrature points,

but rather at only a relatively small representative sampling, where the sequence of configurations are distributed according to $|\Psi_\lambda|^2/\langle\Psi_\lambda|\Psi_\lambda\rangle$. We use Metropolis algorithm³³ which ensures that the desired probability distribution is approached asymptotically.

In this article, the generic form of the variational wave function will be different according to the region of the BCS-BEC crossover. Explicit details will be given for each region separately.

1. Variational calculation for weakly interacting fermions

First, let us consider the region in the potential parameters space where, for a given range $b/2$, the amplitude of the potential is so small that no bound states are allowed in the homogeneous two-body problem. There, it is expected that the trapped ideal Fermi gas configuration gives a rough description of the system. Accordingly, a Jastrow-Slater wave function of the form

$$\Psi_\lambda^{JS} = \Phi_{IFG} \cdot F_\lambda^J \quad (14)$$

is assumed. Here λ is a variational parameter, Φ_{IFG} is the Fermi gas wave function given by the product of Slater determinants (one for each hyperfine state) describing a noninteracting system of harmonically trapped atoms, and the Jastrow function F_λ^J will explicitly include the effects of the interaction potential. It is expected that this kind of wave function gives an appropriate description of the weakly interacting Fermi gas in the normal regime but not in the superfluid one.

The inputs of the Slater determinants are the single-particle eigenstates of a non-interacting particle in a harmonic trap, $\phi_{\mathbf{n}}^{ho}(\mathbf{r})$, with quantum numbers \mathbf{n} at the position \mathbf{r} . This construction ensures that the wave function is totally antisymmetric under the exchange of identical atoms. The energy of each single particle state is characterized by three integer quantum numbers $\mathbf{n} \equiv (n_x, n_y, n_z)$:

$$E_{\mathbf{n}} = \hbar\omega\left(\frac{3}{2} + n_x + n_y + n_z\right), \quad (n_i = 0, 1, 2, \dots) \quad (15)$$

Writing $n = n_x + n_y + n_z$, the degeneracy of each energy level is $(n+1)(n+2)/2$. A typical basis state has the form:

$$\phi_{n_x, n_y, n_z}^{ho}(\mathbf{r}) = \left(\frac{1}{a_{ho}^2 \pi}\right)^{3/4} \prod_{\xi=x,y,z} \frac{H_{n_\xi}(\xi/a_{ho})}{\sqrt{2^{n_\xi} n_\xi!}} e^{-\xi^2/2a_{ho}^2}, \quad (16)$$

where $H_{n_\xi}(\xi/a_{ho})$ are the Hermite functions of order n_ξ and $a_{ho} = \sqrt{\hbar/m\omega}$. In this paper, we consider closed shell configurations so that the ground state is built up by taking all single-particle states with energies increasing from $E_0 = 3\hbar\omega/2$ up to the Fermi energy $E_F = (\mathcal{M}_F + 3/2)\hbar\omega$, where \mathcal{M}_F is the maximum energy level for a given number of particles. For large N , $E_F \sim (6N)^{1/3}\hbar\omega$ and the corresponding radius is $R_F^2 = 2E_F/m\omega^2$.

In the literature of interacting bosons and fermions, the Jastrow wave function usually takes the form of a product $\prod_{i,j} f_{ij}$ of correlation functions f that depend on the degrees of freedom of the pair i, j of interacting particles. In Refs.^{11,25,26,27} f is a function of the interparticle distance r that solves the free-space interacting two-body problem up to a healing distance d after which it is restricted to become constant. In those works, the parameter d is chosen by minimizing the energy.

In this paper, we shall consider trial many-body wave functions which yield a continuous F_λ^J and continuous derivatives; the optimal variational parameter λ of the trial wave function for the many-body system will establish an effective d as we illustrate below. In fact, we have studied two options for the Jastrow function:

(i) $f_{ij} = \exp(-\lambda_{J1} V_0 e^{-2r_{i,j}/b})$, so that,

$$F_{\lambda_{J1}}^J = \exp\left[-\lambda_{J1} \sum_{i_\uparrow, j_\downarrow} V(|\mathbf{r}_{i_\uparrow} - \mathbf{r}_{j_\downarrow}|)\right] \quad (17)$$

(ii)

$$f_{ij} = J_0(z_0 e^{-r_{i,j}/\lambda_{J2}})(1 + c e^{-2r_{i,j}/\lambda_{J2}})P(r_{i,j}/\lambda_{J2})/r_{i,j} \quad (18)$$

The first choice of the variational wave function (17) has the advantage of becoming exact when no interactions between hyperfine states are allowed ($\lambda_{J1} = 0$) which is the trapped ideal Fermi gas limit, where the only correlations are those imposed by the Pauli exclusion principle. It is inspired on previous calculations for the nuclear matter^{28,29}, where an appropriate choice of the potential allows to explore dynamically the interplay of the nuclear-to-quark matter

regime. In addition, this form of the variational wave function allows to estimate the energy expectation value by computing only spatial dependent functions in a Monte Carlo simulation³⁰, with no need of calculating the spatial derivatives of the trial wave function, as we show below.

The second choice is inspired on the general structure of the two-body wave functions in free space at low energies, Eq. (9). It allows to numerically explore shorter potential ranges than the first option (17). It reproduces the fact, first noticed in BCS theories, that even the slightest interaction can lead to two-body long-range-correlations, implicit in the polynomial $P(r_{ij}/b)$. Besides, it increases the reproducibility of interaction effects at short interparticle separations through the factor proportional to c . Deviations from $\lambda_{J2} = b$ should be interpreted as a many-body effect.

The structure of the variational wave function for the BCS region, allows to simplify the expectation value of the kinetic energy operator through an integration by parts²⁸, so that

$$\frac{\langle \Psi_{\lambda_J} | H_{trap} | \Psi_{\lambda_J} \rangle}{\langle \Psi_{\lambda_J} | \Psi_{\lambda_J} \rangle} = E_{IFG} + 2 \sum_{i=1}^N \sum_{j,j'=1}^N \frac{\hbar^2}{2m} \frac{\langle \Psi_{\lambda_J} | \nabla_i(\log f_{ij}) \cdot \nabla_i(\log f_{ij'}) | \Psi_{\lambda_J} \rangle}{\langle \Psi_{\lambda_J} | \Psi_{\lambda_J} \rangle}, \quad (19)$$

where E_{IFG} is the energy of the $2N$ non-interacting trapped Fermi atoms. For closed shell configurations, this energy can be computed using the following equation³¹

$$\frac{E_{IFG}}{2N} = \frac{3}{4} [\mathcal{M}_F + 2] \hbar\omega, \quad (20)$$

instead of the large N limit, $E_{IFG}/2N = 3\mathcal{M}_F\hbar\omega/4$, which produces a slightly underestimated value. Eq. (20) is valid in general. The extra term in Eq. (19) reflects the increase in the kinetic energy of the system, relative to the Fermi-gas estimate, due to interactions.

In the case of Eq. (17), we define the factors $\mathcal{W}_{\lambda_{J1}}$ and $\mathcal{V}_{\lambda_{J1}}$ through the equations

$$\begin{aligned} \sum_{i=1}^N \sum_{j,j'=1}^N \frac{\hbar^2}{2m} \langle \Psi_{\lambda_{J1}} | \nabla_i(\log f_{ij}) \cdot \nabla_i(\log f_{ij'}) | \Psi_{\lambda_{J1}} \rangle &= \frac{\lambda_{J1}^2 \hbar^2}{2m} \sum_{i=1}^N \langle \Psi_{\lambda_{J1}} | \sum_{j,j'=1}^N \nabla_i V(r_{ij}) \cdot \nabla_i V(r_{ij'}) | \Psi_{\lambda_{J1}} \rangle \\ &\equiv \lambda_{J1}^2 \mathcal{W}_{\lambda_{J1}} \langle \Psi_{\lambda_{J1}} | \Psi_{\lambda_{J1}} \rangle, \end{aligned} \quad (21)$$

and

$$\sum_{ij} \langle \Psi_{\lambda_{J1}} | V(r_{ij}) | \Psi_{\lambda_{J1}} \rangle \equiv \mathcal{V}_{\lambda_{J1}} \langle \Psi_{\lambda_{J1}} | \Psi_{\lambda_{J1}} \rangle, \quad (22)$$

so that the expectation value of the total energy is:

$$E(\lambda_{J1}) = E_{IFG} + 2\lambda_{J1}^2 \mathcal{W}_{\lambda_{J1}} + \mathcal{V}_{\lambda_{J1}}. \quad (23)$$

The two functions that remain to be evaluated ($\mathcal{W}_{\lambda_{J1}}$ and $\mathcal{V}_{\lambda_{J1}}$) are local; their expectation values may be computed via Monte Carlo techniques as described above. A similar approach can be used in the case corresponding to the Jastrow function Eq. (18).

We have performed calculations of the energy for a fixed value of N , the range $b/2$ and the scattering length a , exploring for several values of the variational parameter, picking up the one which minimizes the energy. Each run used about 10^3 steps for thermalization and about 10^4 more to take data. In the first rows of Table I, we report the numerical optimal energies using the first choice for the Jastrow function and a potential range $b/2 = 0.015\sqrt{\hbar/m\omega}$. Similar results are obtained when the second choice of F^J is used. The data corresponds to $N = 165$, which fills eight shells ($\mathcal{M}_F = 8$) for the harmonic potential in three dimensions; k_F represents the Fermi wave number associated to the ideal Fermi energy $E_F = (\hbar k_F)^2/2m$. For $N = 165$ the corresponding energy per particle for an ideal Fermi gas is $E_{IFG}/2N = 7.5\hbar\omega$, while $k_F = (2\mathcal{M}_F + 3)^{1/2}\sqrt{m\omega/\hbar} \sim 4.3589\sqrt{m\omega/\hbar}$. The quoted error bars take into account the minimization process itself as well as effects of the initial conditions that could not be erased during the thermalization process. It is important to point out that the variational energy for the highest $1/k_F a$ value coincides with that obtained from a perturbative calculation using a contact interaction as can be verified from expressions obtained in Ref.³¹.

The optimal value of the variational parameter determines the shape of the Jastrow correlation function. As an illustration, in Fig. 4 we plot the behavior of the optimal two particle function f_{ij} of Eq. (17) for $b = 0.03\sqrt{\hbar/m\omega}$ and two different values of the scattering length $1/k_F a = -0.3873$ and -15.8888 respectively. We observe that the distance at which $f_{ij} \sim 1$ is larger than the potential range, this suggests long distance correlated pairs, as expected

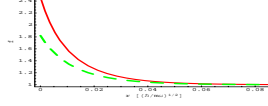


FIG. 4: (Color online) First choice Jastrow correlation function for $b = 0.03\sqrt{\hbar/m\omega}$, dashed and solid lines correspond to $1/k_F a = -0.3873$ and -15.8888 respectively. Distances are measured in units of $\sqrt{\hbar/m\omega}$.

for a BCS-like pairs. This result is also in good agreement with previous findings reported in^{11,26} where the healing distance is used as a variational parameter.

As a approaches the crossover region it is expected that the trial function Eq. (14) will not describe properly the interatomic correlations: pairing effects become essential so that the quantum numbers in the Slater determinants in Φ_{IFG} are not representative of the physical situation.

2. Variational calculation on the BCS-BEC crossover region

In a theory originally put forth by Eagles³⁶ and later by Leggett³⁷, it was proposed that a BCS wave function of the form

$$\Psi_{\lambda_{EL}} = \mathcal{A}[\phi(1_{\uparrow}, 1_{\downarrow})\phi(2_{\uparrow}, 2_{\downarrow})\dots\phi(N_{\uparrow}, N_{\downarrow})], \quad (24)$$

with \mathcal{A} the antisymmetrizer operator that ensures the correct properties under particle exchanges, was more generally applicable than just to the weakly interacting limit³⁶: a BCS-like wave function could eventually describe the ground state from a Cooper pairing region to a BEC of composite bosons made up of two fermions.

Following this point of view, here we propose a family of single-parameter variational wave functions for the BCS-BEC crossover regime, taking $\phi(i_{\uparrow}, j_{\downarrow})$ as a variational extrapolation of the ground state solution of the trapped two body problem

$$\phi(\mathbf{r}_{i\uparrow}, \mathbf{r}_{j\downarrow}) \cong \varphi(r_{i,j})e^{-\lambda_{EL}|\mathbf{r}_{i\uparrow} + \mathbf{r}_{j\downarrow}|^2/4}. \quad (25)$$

The variational parameter λ_{EL} modulates the optimal shape of the cloud. The wave function (24) using the basis (25) guarantees that the Monte Carlo dynamics will be guided by effects of both paired-particles relative $\mathbf{r}_{ij} = \mathbf{r}_{i\uparrow} - \mathbf{r}_{j\downarrow}$ and center of mass $\mathbf{R}_{ij} = (\mathbf{r}_{i\uparrow} + \mathbf{r}_{j\downarrow})/2$ vectors.

It is worth to mention that at difference with previous calculations^{11,13} here, by explicitly including easy interpretable inhomogeneous features in the wave function, we are able to explore the *trapped* atoms as a whole as they evolve into the interacting regime. Besides, at difference with the mean field approach, no optimal individual particle wave functions are searched, but the global effect of the interaction on the paired-particles wave function.

To estimate the energy in the BEC side, the algorithm described for the BCS region is not useful because it depends on the explicit structure of the wave function, written in a Jastrow-Slater form. In order to set the variational energy in a form suitable for Monte Carlo estimations we exploit the two-body structure of the potential and the primitive wave functions ϕ . The antisymmetrized wave function (24) can be explicitly written as

$$\Psi_{\lambda_{EL}} = \sum_{\mathcal{P}} (-1)^{\mathcal{P}} \prod_{i=1}^N \phi(i, \mathcal{P}(i)), \quad (26)$$

where the summation is taken over all possible permutations \mathcal{P} on set \downarrow , and $\phi(i, \mathcal{P}(i))$ are wave functions having the form of Eq. (25) and argument $(\mathbf{r}_{i\uparrow}, \mathbf{r}_{\mathcal{P}(i)\downarrow})$. We can split the Hamiltonian of the system in a pair-like sum, using the center of mass and relative coordinates of possible pairs as:

$$\begin{aligned}
H &= \sum_i^N \left[\frac{p_{i,\mathcal{P}_0(i)}^2}{2\mu} + \frac{\mu}{2} \omega^2 r_{i,\mathcal{P}_0(i)}^2 \right. \\
&\quad + V_{i,\mathcal{P}_0(i)}(r_{i,\mathcal{P}_0(i)}) + \frac{P_{i,\mathcal{P}_0(i)}^2}{2M} + \frac{M}{2} \omega^2 R_{i,\mathcal{P}_0(i)}^2 \Big] \\
&\quad + \sum_{i,j \neq \mathcal{P}_0(i)} V(r_{i,j})
\end{aligned} \tag{27}$$

with \mathcal{P}_0 any given permutation.

Equation (25) let us write:

$$\begin{aligned}
H\Psi_{\lambda_{EL}} &= \left[N\epsilon_0 + N \frac{3\hbar\omega\lambda_{EL}}{2} \right] \Psi_{\lambda_{EL}} \\
&\quad + (1 - \lambda_{EL}^2) \sum_{i,\mathcal{P}} (-1)^{\mathcal{P}} \frac{M}{2} \omega^2 R_{i,\mathcal{P}(i)}^2 \prod_{l=1}^N \phi(l, \mathcal{P}(l)) \\
&\quad + \sum_{\mathcal{P}} (-1)^{\mathcal{P}} \sum_{i,j \neq \mathcal{P}(i)} V(r_{i,j}) \prod_{l=1}^N \phi(l, \mathcal{P}(l))
\end{aligned} \tag{28}$$

with ϵ_0 the ground state eigenvalue of the two body-problem. To evaluate the last two terms via a Monte Carlo simulation we proceed to complete the potential by adding and subtracting the term used in the two-body solution, then:

$$\begin{aligned}
H\Psi_{\lambda_{EL}} &= \left[N\epsilon_0 + N \frac{3\hbar\omega\lambda_{EL}}{2} + \sum_{i,j} V(r_{i,j}) \right] \Psi_{\lambda_{EL}} \\
&\quad + \sum_{i,\mathcal{P}} (-1)^{\mathcal{P}} \prod_{l \neq i} \phi(l, \mathcal{P}(l)) \cdot \left[(1 - \lambda_{EL}^2) \frac{M}{2} \omega^2 R_{i,\mathcal{P}(i)}^2 \right. \\
&\quad \left. - V(r_{i,\mathcal{P}(i)}) \right] \phi(i, \mathcal{P}(i))
\end{aligned} \tag{29}$$

which can also be written in terms of the minors $C_{i\alpha}(\Psi_{\lambda_{EL}})$ associated to the $\Psi_{\lambda_{EL}}$:

$$\Psi_{\lambda_{EL}} = \sum_{\alpha=1}^N C_{i\alpha}(\Psi_{\lambda_{EL}}) \phi_{i,\alpha} \tag{30}$$

where $\phi_{i,\alpha}$ represents any of the i -row wave functions.

$$\begin{aligned}
H\Psi_{\lambda_{EL}} &= \left[N\epsilon_0 + N \frac{3\hbar\omega\lambda_{EL}}{2} + \sum_{i,j} V(r_{i,j}) \right] \Psi_{\lambda_{EL}} \\
&\quad + \sum_{i,\alpha} C_{i,\alpha} \cdot \left[(1 - \lambda_{EL}^2) \frac{M}{2} \omega^2 R_{i,\alpha}^2 - V(r_{i,\alpha}) \right] \phi(i, \alpha)
\end{aligned}$$

This expression results quite convenient for the simulations to be performed, where one can also take advantage from the relation between minors and the elements of the inverse of the transposed matrix³⁰,

$$\bar{\phi}_{i,\alpha} \equiv (\phi^T)_{i\alpha}^{-1} = \frac{C_{\alpha,i}(\Psi_{\lambda_{EL}}^T)}{\Psi_{\lambda_{EL}}^T} = \frac{C_{i,\alpha}(\Psi_{\lambda_{EL}})}{\Psi_{\lambda_{EL}}}. \tag{31}$$

Thus, we can write

$$\begin{aligned}
H\Psi_{\lambda_{EL}} &= \left[N\epsilon_0 + N \frac{3\hbar\omega\lambda_{EL}}{2} + \sum_{i,j} V(r_{i,j}) \right. \\
&\quad \left. + \sum_{i,\alpha} \phi_{i,\alpha} \bar{\phi}_{i,\alpha} \left[(1 - \lambda_{EL}^2) \frac{M}{2} \omega^2 R_{i,\alpha}^2 - V(r_{i,\alpha}) \right] \right] \Psi_{\lambda_{EL}}
\end{aligned} \tag{32}$$

As in the BCS calculation, we can sample the system using a Metropolis-Monte Carlo algorithm and estimate the energy as a function of the variational parameter.

In Table I, we illustrate the results on the optimal variational parameter and different energy estimates for several scattering lengths. The strength of the potential was taken in the region around the first zero-resonance condition $(z_0/b)^2 \hbar\omega = \tilde{v}_0$. The upper set of results were obtained using the Jastrow-Slater wave function Eqs. (14,17). All other results considered a wave function of the Eagles-Leggett form, Eq. (24), with the two-body functions Eq. (25) taking $\varphi(r_{i,j})$ as the approximate solutions of the two-body problem for a given scattering length, Eqs.(9-10).

In the reported calculations using Eagles-Leggett wave functions, the range of the potential was taken as $b/2 = 0.00375\sqrt{\hbar/m\omega}$ before the unitarity limit, $1/k_F a = 0$, and $b/2 = 0.0025\sqrt{\hbar/m\omega}$ for $k_F a \geq 0$. Actually, calculations were performed for several potential ranges $b/2$ all over the crossover. The $b/2$ ranges reported in this table are the shortest for which reliable numerical results were obtained.

For $1/k_F a < -0.45$ the variational energy $E/2N$ for the wave-function (24-25) is higher than that obtained with the Jastrow-Slater trial wave-function, while for $1/k_F a > -0.45$ the situation is inverted and the *BCS*-wave function gives a lower upper bound for $E/2N$. A similar effect has been found in Ref.¹³ for the homogeneous gas. Beyond the unitarity region, *i. e.* for $a > 0$, the contribution $\epsilon_0/2$ coming from the trapped ground state two-body eigenvalue has been subtracted. For $4 < 1/k_F a < 12$ an optimal value of $\lambda_{EL} \sim 1$ yielding a local minimum was found. However, for $\lambda_{EL} > 1$ the corresponding mean value of the energy can be made arbitrarily small by considering λ_{EL} large enough. This variational instability is expected at the extreme BEC region for any attractive potential of *finite* range as discussed previously in Ref.¹² for a homogeneous gas. It could eventually be avoided by adding a repulsive interaction at distances much smaller than the range $b/2$ as suggested in the original work by Leggett³⁷. Implementing this idea within our numerical approach is very difficult since we have already set $b \ll \sqrt{\hbar/m\omega}$. Although a local minimum was found for $1/k_F a > 4$, finite range effects are expected to be significant on the reported data.

The wave function having $\lambda_{EL} \sim 1$ is expected for a molecular gas when Pauli Blocking effects between the constituting fermionic atoms are approximately compensated by the attractive finite range interaction effects. If the atoms did not interact, the corresponding energy per atom would be $E/2N = 1.5\hbar\omega$ corresponding to an ideal gas of trapped Bose molecules. It is also important to emphasize that, for a *contact* interaction, molecules formed by Fermi atoms are expected to have a weakly repulsive interaction, with a molecule-molecule scattering length given by $a_{mm} = 0.6a$ ³⁸.

3. Virial relations

In the fifth column of Table I, we also report $\langle m\omega^2 R^2 \rangle$, that is, twice the mean value of the trapping potential energy per particle, which is more feasible of experimental verification²⁰ than the total energy E . Notice that in the crossover region with $-0.1 < 1/k_F a < 1.4$, the energies in the third column are similar to $\langle m\omega^2 R^2 \rangle$.

At unitarity, $1/k_F a = 0$, a virial relation of the form $E/2N = \langle m\omega^2 R^2 \rangle$ is expected from previous experimental and theoretical studies^{9,39}. During the revision process of the present article, virial theorems for trapped interacting atoms outside the unitarity limit have been established both at finite temperature^{40,41} and at zero temperature^{42,43}. The latter considered several forms of the interaction potential. In particular for a contact interaction with a strength determined by the scattering length a , it has been shown that:

$$\frac{E}{2N} = \langle m\omega^2 R^2 \rangle - \frac{1}{2} k_F a \frac{\partial E/2N}{\partial k_F a} \quad (33)$$

$$= \langle m\omega^2 R^2 \rangle + \frac{1}{2k_F a} \frac{\partial E/2N}{\partial 1/k_F a}. \quad (34)$$

For a contact interaction in the free space, the energy of the bound state is $\epsilon_0^c = -\hbar^2/ma^2$. So that, $k_F a \partial \epsilon_0^c / \partial k_F a = -2\epsilon_0^c$ and, in the BEC side of the crossover,

$$\langle m\omega^2 R^2 \rangle_{virial}^c = (E/2N - \epsilon_0^c/2) - \frac{1}{2} \left[\frac{1}{k_F a} \frac{\partial (E/2N - \epsilon_0^c/2)}{\partial 1/k_F a} \right]. \quad (35)$$

Although we have made all calculations with a finite range potential we would like to evaluate how compatible our results are with those arising from contact interaction predictions. Thus, in the last column of Table I we report the mean value of twice the potential energy per particle associated to the trap, evaluated numerically using Eq. (34) in the BCS side and the following expression in the BEC side:

$$\langle m\omega^2 R^2 \rangle_{virial}^b = (E/2N - \epsilon_0^b/2) - \frac{1}{2} \left[\frac{1}{k_F a} \frac{\partial (E/2N - \epsilon_0^b/2)}{\partial 1/k_F a} \right] \quad (36)$$

$1/k_F a$	$V_0 \lambda_{J1}^{opt}$ ± 0.05	$E/2N$ [$\hbar\omega$]	ϵ_0 [$\hbar\omega$]	$\langle m\omega^2 R^2 \rangle$ [$\hbar\omega$]	$\langle m\omega^2 R^2 \rangle_{virial}$ [$\hbar\omega$]
-15.88895	-0.6	7.450 ± 0.004	1.49	$7.5^a \pm 0.2$	7.418 ± 0.006
-9.60883	-0.6	7.425 ± 0.005	1.48	$7.5^a \pm 0.2$	7.39 ± 0.0075
-4.26632	-0.6	7.374 ± 0.009	1.46	$7.53^a \pm 0.2$	7.31 ± 0.03
-2.02479	-0.9	7.345 ± 0.012	1.42	$7.53^a \pm 0.2$	7.25 ± 0.03
$1/k_F a$	$\lambda_{EL}^{opt} \hbar/m\omega$ ± 0.005	$E/2N$ [$\hbar\omega$]	ϵ_0 [$\hbar\omega$]	$\langle m\omega^2 R^2 \rangle$ [$\hbar\omega$]	$\langle m\omega^2 R^2 \rangle_{virial}$ [$\hbar\omega$]
-0.43893	0.142	7.07 ± 0.06	1.15	$7.72^a \pm 0.2$	6.88 ± 0.09
-0.22418	0.134	6.65 ± 0.06	0.99	$7.57^a \pm 0.2$	6.42 ± 0.09
-0.10071	0.160	6.37 ± 0.06	0.79	6.58 ± 0.2	6.21 ± 0.09
-0.03745	0.182	6.10 ± 0.06	0.72	5.64 ± 0.2	5.88 ± 0.09
0	0.186	5.25 ± 0.08	0.50	5.32 ± 0.2	5.25 ± 0.12
$1/k_F a$	$\lambda_{EL}^{opt} \hbar/(m\omega)$ ± 0.005	$(E/2N) - \epsilon_0/2$ [$\hbar\omega$]	$-\epsilon_0$ [$\hbar\omega$]	$\langle m\omega^2 R^2 \rangle$ [$\hbar\omega$]	$\langle m\omega^2 R^2 \rangle_{virial}$ [$\hbar\omega$]
0.13959	0.190	4.78 ± 0.07	0.21	4.92 ± 0.2	4.85 ± 0.11
0.34876	0.191	4.18 ± 0.07	2.45	4.50 ± 0.2	4.52 ± 0.11
0.69684	0.256	3.57 ± 0.07	9.95	3.75 ± 0.2	3.95 ± 0.2
1.04427	0.270	3.35 ± 0.06	22.65	3.51 ± 0.2	3.85 ± 0.2
1.39107	0.380	3.14 ± 0.08	40.76	2.99 ± 0.2	3.69 ± 0.2
2.08293	0.665	2.60 ± 0.08	93.96	2.95 ± 0.2	3.38 ± 0.2
2.77266	0.90	2.0 ± 0.1	171.157	2.89 ± 0.2	3.09 ± 0.2
3.46055	0.94	1.38 ± 0.15	274.99	2.59 ± 0.25	2.45 ± 0.23
4.1469	0.99	1.1 ± 0.15	404.64	2.59 ± 0.25	1.71 ± 0.23
5.51634	0.99	0.95 ± 0.15	756.643	2.59 ± 0.40	1.19 ± 0.23

^aThe evaluation of mean radii for extended clouds requires special care of the statistics.

TABLE I: Optimal variational parameter λ , energy per particle, two-body ground ϵ_0 energies, mean value of the trap potential energy per particle $\langle m\omega^2 R^2 \rangle$ from Monte Carlo calculations and $\langle m\omega^2 R^2 \rangle_{virial}$ evaluated using the virial relation given by Eq. (34,36). All of them were calculated as a function of $1/k_F a$ considering $2N = 330$ particles. The upper set of results used the Jastrow-Slater wave function Eqs. (14,17). All other results considered a wave function of the Eagles-Leggett form, Eq. (24), with the two-body functions $\varphi(r_{i,j})$ taken as the approximate solutions of the two-body problem for a given scattering length.

with ϵ_0^b the two particle energy for a finite range interaction state in otherwise free space. The numerical evaluation of the derivative was preceded by a numerical smoothing of data. We observe that, although the calculations were performed using a finite range potential, there is a reasonable agreement between the trap energies and the virial expressions Eqs. (34) and (36) for $-0.1 < 1/k_F a < 3.5$.

It was also found that as $1/k_F a \rightarrow 0^-$ and $1/k_F a \rightarrow 0^+$ the derivatives in Eq. (34) and Eq. (36) respectively attain a minimum. This minimum together with the small difference between the value of $\epsilon_0/2$ and $\epsilon_0^b/2$ compared to $E/2N$ for $0 < 1/k_F a < 1.5$, let us understand the observed similarities between the third, fifth and sixth columns of Table I for $-0.1 < 1/k_F a < 1.4$.

On the BCS side of the crossover, for $-0.5 < 1/k_F a < -0.2$, our wave functions yield a 15% higher trapping energy than the virial relation predicts. It is important to mention that, for these values of $1/k_F a$, the atomic cloud is quite extended and the evaluation of both the mean energy $E/2N$ and the mean square radius $\langle R^2 \rangle$ requires special care of the statistics sampling. Improving the form of the variational wave function in this region, could diminish the discrepancy with the virial relation. Notice that, in the language of BCS theory, these region delimits the transition of the atomic cloud from a normal to a superfluid state.

In the region $1/k_F a > 4$ there is also a discrepancy with the contact virial relation; it could be due to finite range potential effects as expected from the variational instability reported above. In fact, for these scattering lengths the difference between atoms interacting through a contact and a finite range potential is already evident by comparing their corresponding two-body ground state energies ϵ_0 . These energies are in general similar but, as expected, the bigger differences appear for the deeply bound two-body states, $a \rightarrow 0^+$. For instance, at the bottom of Table I, $\epsilon_0 = -756.6\hbar\omega$ in contrast to the solution of Eq. (8) which yields $-578.1\hbar\omega$; for the other states the difference is less than 10% up to $1/k_F a < 2.5$ and around 15% for the remaining reported data.

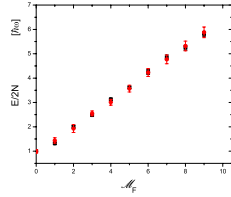


FIG. 5: (Color online) s -ground state variational energy per atom $E/2N$ and $\langle m\omega^2 R^2 \rangle$ for trapped particles at unitarity as a function of the Fermi number \mathcal{M}_F for closed shells. Energy is measured in units of $\hbar\omega$.

4. Unitarity

At unitarity, $|a| \rightarrow \infty$, we have estimated the energy using a variational wave function of the form Eq. (26). The numerical results were presented and broadly discussed in Ref.²¹ in connection with the universality hypothesis. Notice that, in Table I, the numerical errors at unitarity are slightly larger than those obtained for nearby scattering lengths. The reason can be traced back to the qualitative difference between the two-body wave function $u_{ij} = r\varphi_{ij}$ determined by Eq. (10). The high delocalization of the unitarity paired-atoms wave function makes more difficult the evaluation of the energy expectation value at this limit. From these results, an upper bound to the universal parameter β , defined by $E_U = E_{IFG}\sqrt{1+\beta}$, is found to be $\beta = -0.51 \pm 0.01$.

In Fig. 5, we show the mean value $\langle m\omega^2 R^2(\mathcal{M}_F) \rangle$ together with $E(\mathcal{M}_F)$ for closed shells with $\mathcal{M}_F \leq 9$ corresponding to $N = 4, 10, 20, 35, 56, 84, 120, 165$ and 220 particles. No significant discrepancy among these mean values is observed and the virial relation is thus verified. As reported in Ref.²¹, a linear relationship between the energy per particle at unitarity and the shell number \mathcal{M}_F is also found:

$$E_U/2N \sim (0.53 \pm 0.01)(\mathcal{M}_F + (1.95 \pm 0.06))\hbar\omega, \quad (37)$$

when this expression is compared with the ideal Fermi gas result, Eq. (20), one obtains an upper bound for the universal parameter $\beta = -0.50^{(+0.02)}_{(-0.04)}$.

B. Densities and correlations

The information encoded in the single-particle and the two-particle correlation functions is important since those functions reflect the quantum mechanical nature of the particles and their collective behavior, driven by the interaction and trapping potentials.

In the following, we illustrate these correlation functions for $N = 165$ using the optimized wave functions in the BCS ($a < 0$), the unitarity ($a \rightarrow \infty$) and the molecular ($a > 0$) regimes. We have chosen examples in the crossover with $|1/k_F a| < 1$ due to its expected independence on the details of the calculation.

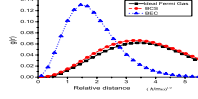


FIG. 6: (Color online) Normalized correlation function $g(r)$ for particles in the same hyperfine state as a function of their relative distance. Square, circle, and triangle symbols correspond to the ideal Fermi gas, BCS ($1/k_F a = -0.224$) and BEC ($1/k_F a = 0.697$) respectively. Distances are measured in units of $\sqrt{\hbar/m\omega}$.

For completeness, let us recall that the single-particle correlation function, that is, the density profile as a function of the distance to the center of the harmonic trap, has already been illustrated in Fig. 2 of Ref.²¹. There, we saw that the trap effect is reflected by decreasing the particle density until vanishing around the Fermi radius, i.e., the inhomogeneous environment created by the harmonic confinement affects all the regimes as it is already evident for an ideal Fermi gas in the Thomas-Fermi approximation³⁵. The shape of the BCS density profile is similar to the one corresponding to the ideal gas but with a different mean radius. The density increases at the center while decreases as it goes to the edge of the trap. These deviations can be attributed to the optimal value of the variational parameter which captures the interaction and correlation effects in the many-body system. This kind of shape prevails up to the unitarity limit. The major differences in the particle density for each regime occur around the center of the trap, particularly for the BEC regime where most of the paired atoms are located near the origin.

In order to exhibit the quantum behavior of the fermionic atoms, the two-particle correlation function for particles in the same hyperfine state, $g(r)$, was computed. The calculations involved finding the fraction of atoms in the same hyperfine state within a relative distance $(r, r + dr)$, as generated by the Monte Carlo sampling, irrespective of the center of mass position; $g(r)$ was normalized dividing by $N(N-1)/2$ to account for the combinatorial of the atoms. Figure 6 illustrates the resulting correlation functions. The Jastrow-Slater wave function in the limit of an ideal Fermi gas ($\lambda_{J1} = 0$), exhibits the Pauli blocking arising from the fermionic nature of the atoms. The BCS trial wave function shows an slightly diminished Pauli blocking for short distances. In the molecular side, it is observed that particles in the same hyperfine state can be found around the same region. Although at the deep BEC regime Pauli blocking still inhibits the presence of atoms in the same hyperfine state, the radius at which it is evident becomes very short. As a consequence, if an exclusively attractive interacting potential is considered and it is large enough, Pauli blocking is not able to avoid a variational collapse as discussed above. All of these correlations decrease for long relative distances as a consequence of the presence of the trap.

The two-particle correlation function for atoms in different hyperfine states was computed in Ref.²¹. There (Fig. 3) its behavior in the BEC regime is compared with respect to the ideal regime, as a function of the relative distance $r_{i,j} = |\mathbf{r}_{i\uparrow} - \mathbf{r}_{j\downarrow}|$ among them. It was evaluated in a similar way to $g(r)$, taking care of the proper normalization factor (N^2) and keeping the information of the center of mass position of the pairs. Molecule formation was indicated by the increase in the correlation for very short distances, $r_{i,j} \ll \sqrt{\hbar/m\omega}$. Most molecules are formed for $R_{cm} < 1.09\sqrt{\hbar/m\omega}$. An enhancement of the probability of finding pairs of particles separated at relative distances of the order of $r_{i,j} \sim \sqrt{\hbar/m\omega}$ indicated molecular condensation effects.

Here, in Fig. 7 we illustrate the differences between the two-particle correlation functions of atoms in different hyperfine states, $\Delta K(r_{i,j}, R_{cm})$ for the ideal and BCS regimes. As in Fig. 3 of Ref.²¹, it shows results for a set of radius R_{cm} measured from the center of the trap. We observe that, although not zero, the difference is very small (see the abscissa scale) compared to the result for the BEC regime, in addition strong oscillations in $r_{i,j}$ are seen for all R_{cm} .

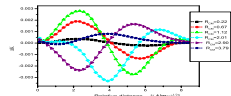


FIG. 7: (Color online) Probability difference $\Delta K(r_{i,j}, R_{cm})$ that two particles with different spin are found separated a distance $r_{i,j}$ in the BCS and ideal regimes. Each curve in this figure correspond to a spherical radius R_{cm} measured from the center of the trap. Calculations are performed at $1/k_F a = -0.224$. Distances are measured in units of $\sqrt{\hbar/m\omega}$.

IV. CONCLUSIONS

We have studied an interacting two-component Fermi gas confined in an isotropic harmonic potential in three dimensions. To be specific, we investigated the transition from a Bardeen-Cooper-Schrieffer state to a Bose-Einstein condensate at zero temperature for a system composed of $N = 165$ particles of equal mass in each spin-state. The interaction between particles of different spin was considered to be an attractive potential with very short range interaction; under such conditions it is expected that the many-body ground state depends just on the product of the scattering length a and the Fermi wave number k_F . The BCS-BEC transition was followed as a function of $k_F a$.

To model the gas, we proposed a family of many-body trial wave functions for the BCS ($a < 0$) and the BEC ($a > 0$) sides. For small negative values of a we described the atomic gas by a Jastrow-Slater wave function. While, for other values of a , following Eagles and Leggett proposal, a wave function written as the antisymmetric product of two-particle states was used. The two-body basis was formed by analytical compact functions that contain collision and trapping effects. For a given interaction range, using variational Quantum Monte Carlo simulations, we found the variational parameter λ^{opt} that minimizes the energy per particle of the whole system. Efficient algorithms to estimate the energy expectation value, exploiting properties of the antisymmetrized many-body functions, were elaborated to perform calculations for such a large number of particles. After considering several values of the range of the potential and studying the stability of the results, we reported the numerical data corresponding to the lowest value of the potential range that gave reliable numerical results. The corresponding optimal variational wave functions lead to predictions for the main properties of the trapped system like energies, mean squared radii, one and two-point correlation functions.

The system energy was computed all along the crossover, and at unitarity an upper bound to the universal parameter β is found to be $\beta = -0.51 \pm 0.01$. This result is compatible with the result reported in Ref.²¹ where $\beta_{fit} = -0.50_{+0.04}^{-0.02}$ was found by comparing E_U and E_{IFG} for $\mathcal{M}_F \leq 9$. Those calculations indicate that the universal hypothesis yields results consistent with theoretical calculations even for a small N . So that, for zero temperature, the energy of a balanced mixture of interacting trapped fermions has the form $E_U \sim 1/2(\mathcal{M}_F + 2)2N\hbar\omega$ similar to the ideal Fermi gas equation $E_{IFG} = 3/4(\mathcal{M}_F + 2)2N\hbar\omega$. In addition it was shown that not only at unitarity but also over the crossover region $-0.1 < 1/k_F a < 1.4$ the mean value of the atomic gas squared radius can be used to give a rough estimate of the energy per particle, since $\langle m\omega^2 R^2 \rangle \sim E/2N - \bar{\epsilon}_0/2$, where $\bar{\epsilon}_0$ is the two-body ground state energy ϵ_0 for trapped fermions for $a > 0$ and zero for $a \leq 0$ and $|a| \rightarrow \infty$.

In agreement with previous results²¹, the energy function $E(1/k_F a)$ along the crossover follows a curve that properly normalized is independent of \mathcal{M}_F . By evaluating its numerical derivative a minimum was found at unitarity. Besides, this function was shown to satisfy a virial relation in the interval $-0.1 < 1/k_F a < 3.4$. This relation was based on virial theorems for trapped atoms developed by other groups in the last few months^{40,41,42,43}.

The starting point of the crossover from the BCS side could be regarded as the value of $1/k_F a$ for which the antisymmetric product of two-particle states gives a lower expectation value of the energy with respect to the Jastrow-Slater wave function. According to our calculations this already occurs at $1/k_F a \sim -0.45$. This value is similar to that at which a variational calculation based on scaled antisymmetric product of harmonic oscillator wave functions can not be applied since no minima exists³¹. Although the Eagles-Leggett wave function, built using the solutions of the two-body problem, gives a better description of the system than its Jastrow-Slater analog, it yields a mean radius

for the atomic cloud 15% larger than that predicted by the virial relations. Thus, it would be important to work out an improved trial wave function to describe this transition zone.

In the extreme BEC region there is a variational instability which arises from the usage of *finite* range attractive potentials between the fermions. In our calculations the extreme BEC region starts when the variational parameter λ_{EL} yields a local minimum energy for $\lambda_{EL}^{opt} > 1$. In such a case the effect of Pauli blocking is superseded by the very strong short range attractive potential. For $12 > 1/k_F a > 3.5$ and $b/2 = 0.0025\sqrt{\hbar/m\omega}$ a local minimum was found with $\lambda_{EL} \sim 1$. This value of λ_{EL} corresponds to a many-body wave function of an ideal Bose gas of trapped molecules. This function does not satisfy the virial relation for a contact interaction so that even though $b/2 \ll \sqrt{\hbar/m\omega}$, finite range effects are not negligible for those values of $k_F a$.

Finally, we calculated the one-particle and the two-particle correlation functions for the BCS and BEC regimes and for the unitary limit. The results show that the correlation length between pairs can be much larger than the interaction potential range. As expected, the inhomogeneous environment resulting from the harmonic confinement affects all the regimes. We observe that in the BCS regime, the paired atoms have a large correlation length particularly for $0.6 < R_{cm} < 1.2\sqrt{\hbar/m\omega}$. Pauli blocking effects were also sensible to trapping and interaction strength. Thus, we conclude that the approximate analytical wave function used to describe the trapped interacting gas gives a good compact representation of the system through the crossover region.

Acknowledgments This work was partially supported by Conacyt México, under grant 41048-A1 and DGAPA-UNAM contract PAPIIT IN117406-2.

-
- ¹ B. DeMarco and D. S. Jin, Science **285**, 1703 (1999).
 - ² S. Jochim, M. Bartenstein, A. Altmeyer, G. Hendl, S. Riedl, C. Chin, J. H. Denschlag, and R. Grimm, Science **302**, 2101 (2003); M. Greiner, C. A. Regal, and D. S. Jin, Nature **426**, 537 (2003); M. W. Zwierlein, C. A. Stan, C. H. Schunck, S. M. F. Raupach, S. Gupta, Z. Hadzibabic, and W. Ketterle, Phys. Rev. Lett. **91**, 250401 (2003); K. E. Strecker, G. B. Partridge, and R. G. Hulet, Phys. Rev. Lett. **91**, 080406 (2003).
 - ³ K. M. O'Hara, S. L. Hemmer, M. E. Gehm, S. R. Granade, J. E. Thomas, Science **298**, 2179(2002); M. E. Gehm, S. L. Hemmer, S. R. Granade, K. M. O'Hara, and J. E. Thomas, Phys. Rev. A **68**, 011401(R) (2003).
 - ⁴ M. Bartenstein, A. Altmeyer, S. Riedl, S. Jochim, C. Chin, J. H. Denschlag, and R. Grimm, Phys. Rev. Lett. **92**, 120401 (2004).
 - ⁵ T. Bourdel, J. Cubizolles, L. Khaykovich, K. M. F. Magalhaes, S. J. J. M. F. Kokkelmans, G. V. Shlyapnikov, and C. Salomon, Phys. Rev. Lett. **91**, 020402 (2003).
 - ⁶ T. Bourdel, L. Khaykovich, J. Cubizolles, J. Zhang, F. Chevy, M. Teichmann, L. Tarruell, S.J.J.M.F. Kokkelmans, and C. Salomon, Phys. Rev. Lett. **93**, 050401 (2004).
 - ⁷ H. Heiselberg, Phys. Rev. A **63**, 043606 (2001).
 - ⁸ T.-L. Ho, Phys. Rev. Lett. **92**, 090402 (2004).
 - ⁹ F. Werner and Y. Castin, Phys. Rev. A **74**, 053604 (2006).
 - ¹⁰ W. Vincent Liu, Phys. Rev. Lett. **96**, 080401 (2006).
 - ¹¹ J. Carlson, S. Y. Chang, V. R. Pandharipande, and K. E. Schmidt, Phys. Rev. Lett. **91**, 050401 (2003).
 - ¹² S. Y. Chang, V. R. Pandharipande, J. Carlson, and K. E. Schmidt, Phys. Rev. A **70**, 043602 (2004).
 - ¹³ G. E. Astrakharchik, J. Boronat, J. Casulleras, and S. Giorgini, Phys. Rev. Lett. **93**, 200404 (2004).
 - ¹⁴ D. Lee, Phys. Rev. B **73**, 115112 (2006).
 - ¹⁵ S. Y. Chang and G. F. Bertsch, Phys. Rev. A **76**, 021603(R) (2007).
 - ¹⁶ D. Blume, J. von Stecher, C. H. Greene, Phys. Rev. Lett. **99**, 233201 (2007).
 - ¹⁷ J. von Stecher and C. H. Greene, and D. Blume, Phys. Rev. A **77**, 043619 (2008).
 - ¹⁸ J. Kinast, A. Turlapov, J. E. Thomas, Q. J. Chen, J. Stajic, and K. Levin, Science **307**, 1296 (2005).
 - ¹⁹ G. B. Partridge, W. Li, R. I. Kamar, Y. an Liao, and R. G. Hulet, Science **311**, 503 (2005).
 - ²⁰ J. T. Stewart, J. P. Gaebler, C. A. Regal, and D. S. Jin, Phys. Rev. Lett. **97**, 220406 (2006).
 - ²¹ R. Jáuregui, R. Paredes and G. Toledo Sánchez, Phys. Rev. A **76**, 011604(2007).
 - ²² E. L. Bolda, E. Tiesinga, and P. S. Julienne, Phys. Rev. A **66**, 013403 (2002).
 - ²³ W. Rarita and R. D. Present, Phys. Rev. **51**, 788 (1937).
 - ²⁴ T. Busch, B.G. Englert, K. Rzażewski, and M. Wilkens, Foundations of Phys. **28**, 549 (1998).
 - ²⁵ D. Schiff and L. Verlet, Phys. Rev. **160**, 208 (1967).
 - ²⁶ V. R. Pandharipande and H. A. Bethe, Phys. Rev. C **7**, 1312 (1973).
 - ²⁷ V. R. Pandharipande and K.E. Schmidt, Phys. Rev. A **15**, 2486 (1977).
 - ²⁸ C. J. Horowitz, E. J. Moniz and J. W. Negele, Phys. Rev. D **31**, 1689 (1985); C. J. Horowitz and J. Piekarewicz, Nucl. Phys. A **536**, 669 (1992).
 - ²⁹ G. Toledo Sánchez, and J. Piekarewicz, Phys. Rev. C **65**, 045208 (2002).
 - ³⁰ D. Ceperley, G.V. Chester and M.H. Kalos, Phys. Rev. B **16**, 3081 (1977).
 - ³¹ R. Jáuregui, R. Paredes and G. Toledo Sánchez, Phys. Rev. A. **69** 013606 (2004).

- ³² Steven E. Koonin, “*Computational Physics*” (Benjamin Cummings, Menlo Park, 1986).
- ³³ N. Metropolis, A. Rosenbluth, M. Rosenbluth, A. Teller, and E. Teller, J. Chem Phys. **21**, 1087 (1953).
- ³⁴ G. A. Baker, Phys. Rev. C **60**, 054311 (1999).
- ³⁵ D.A. Butts and D.S. Rokhsar, Phys. Rev. A **55**, 4346 (1997).
- ³⁶ D. M. Eagles, Phys. Rev. **186**, 456 (1969).
- ³⁷ A. J. Leggett, J. Phys. (Paris) **41**, C7 (1980).
- ³⁸ D.S. Petrov, C. Salomon, and G.V. Shlyapnikov, Phys. Rev. Lett. **93**, 090404 (2004).
- ³⁹ J. E. Thomas, J. Kinast, and A. Turlapov, Phys. Rev. Lett. **95**, 120402 (2005).
- ⁴⁰ S. Tan, e-print arXiv:0803.0841.
- ⁴¹ E. Braaten and L. Platter, Phys. Rev. Lett. **100**, 205301 (2008).
- ⁴² J. E. Thomas, Phys. Rev. A **78**, 013630 (2008).
- ⁴³ F. Werner, Phys. Rev. A **78**, 025601 (2008).